Journal of Medicinal Chemistry

Article

pubs.acs.org/jmc

Exploiting the Therapeutic Potential of 8-β-D-Glucopyranosylgenistein: Synthesis, Antidiabetic Activity, and Molecular Interaction with Islet Amyloid Polypeptide and Amyloid β-Peptide (1−42)

Ana R. Jesus,[†] Catarina Dias,[†] Ana M. Matos,[†,‡] Rodrigo F. M. de Almeida,[†] Ana S. Viana,[†] Filipa Marcelo,[∥] Rogério T. Ribeiro,[‡,§] Maria P. Macedo,[‡,§] Cristina Airoldi,[⊥] Francesco Nicotra,[⊥] Alice Martins,[†] Eurico J. Cabrita,[∥] Jesús Jiménez-Barbero,[#] and Amélia P. Rauter*[,†]

[†]Center of Chemistry and Biochemistry, Department of Chemistry and Biochemistry, Faculdade de Ciências, Universidade de Lisboa, Ed C8, Piso 5, Campo Grande, 1749−016 Lisboa, Portugal

[‡]CEDOC Chronic Diseases Center, Faculdade de Ciências Médicas, Universidade Nova de Lisboa, Rua Câmara Pestana, 6, 6ª, 1150-082, Lisboa, Portugal

[§]APDP, Diabetes Portugal Education and Research Center, APDP-ERC, Rua do Salitre, 118-120, 1250-203 Lisboa, Portugal

[∥]REQUIMTE, CQFB, Department of Chemistry, Faculdade de Ciências e Tecnologias, Universidade Nova de Lisboa, Quinta da Torre, 2829-516 Caparica, Portugal

[⊥]Department of Biotechnology and Biosciences, University Milano Bicocca, Piaza della Sciencia 2-4, 20126, Milano, Italy

[#]Centro de Investigaciones Biológicas, C.S.I.C., Ramiro de Maeztu 9, 28040 Madrid, Spain

Supporting Information

ABSTRACT: 8-β-D-Glucopyranosylgenistein (**1**), the major component of *Genista tenera*, was synthesized and showed an extensive therapeutical impact in the treatment of STZ-induced diabetic rats, producing normalization of fasting hyperglycemia and amelioration of excessive postprandial glucose excursions and and increasing β-cell sensitivity, insulin secretion, and circulating insulin within 7 days at a dose of 4 (mg/kg bw)/day. Suppression of islet amyloid polypeptide (IAPP) fibril formation by compound **1** was demonstrated by thioflavin T fluorescence and atomic force microscopy. Molecular recognition studies with IAPP and $A\beta_{1-42}$ employing saturation transfer difference (STD) confirmed the same binding mode for both amyloid peptides as suggested by their deduced epitope. Insights into the preferred conformation in the bound state and conformers' geometry resulting from interaction with $A\beta_{1-42}$ were also given by STD, trNOESY, and MM calculations. These studies strongly support 8-β-D-glucopyranosylgenistein as a promising molecular entity for intervention in amyloid events of both diabetes and the frequently associated Alzheimer's disease.

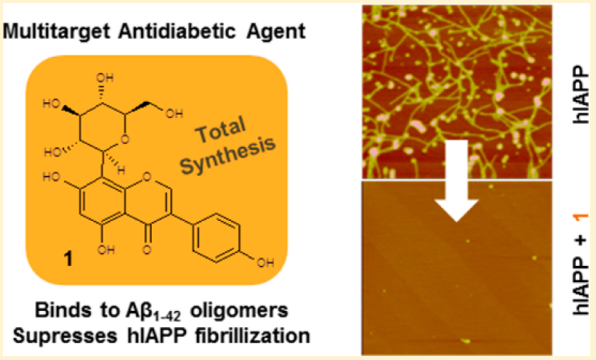

INTRODUCTION

Because of population growth, aging, lifestyle alterations, and increasing prevalence of obesity, the past 2 decades have seen an explosive increase in people diagnosed with *Diabetes mellitus* (DM). Therefore, research on new medicines for the prevention and treatment of this chronic disease remains mandatory. Type 2 DM is caused by a combination of resistance to insulin and impaired insulin secretion, a dysfunction associated with islet amyloid deposits derived from islet amyloid polypeptide (IAPP), a protein coexpressed and secreted with insulin by pancreatic β-cells. This accumulation of amyloid fibrils, also encountered in many other age related degenerative diseases, namely, in Alzheimer's disease (AD), occurs as an outcome of protein misfolding.[1]

Amyloids from different diseases may share a common pathway for fibril formation, since they have common structural properties.[2] In the case of type 2 DM and AD, studies have also shown that both IAPP and Aβ small and soluble oligomers are actually the most toxic aggregates to β-cells and neurons, respectively, when compared to larger amyloid fibrils.[3,4] Thus, targeting these prefibrillar amyloidogenic proteins seems to be a rational approach.

Polyphenolic molecular entities have demonstrated the ability to inhibit the formation of β-amyloid fibrils in vitro and their associated cytotoxicity.[5] In particular, genistein has

Received: July 16, 2014

   dx.doi.org/10.1021/jm501069h | J. Med. Chem. XXXX, XXX, XXX−XXX

the ability to prevent fibrillization and oligomerization and has fibril-destabilizing effects on $A\beta_{1-40}$ and $A\beta_{1-42}$ in vitro.[6] In addition, (−)-epigallocatechin 3-gallate (EGCG)[7,8] and 1,2,3,4,6-penta-*O*-galloyl-β-D-glucopyranose (PGG)[9,10] were reported to inhibit in vitro amyloid formation of both IAPP and Aβ peptides. A dietary supplementation of EGCG for 5 weeks resulted in reduction of blood glucose levels[11] and has proven to delay the onset of type I diabetes,[12] while PGG was found to ameliorate high-fat-diet-induced diabetes in C57BL/6 mice.[13]

The plant kingdom is indeed a valuable source of compounds effective against amyloid disorders, in particular diabetes.[14,15] Our previous results revealed that *Genista tenera*,[16−21] including its ethyl acetate extract, has a promising antidiabetic activity on an STZ-induced diabetic animal model. In vitro toxicity studies showed no evidence for extract acute cytotoxicity or genotoxicity.[21] The O-glycosylated flavonoid components lowered blood glucose levels of STZ induced diabetic Wistar rats,[20] although their activity was not comparable to that of the extract.[21] Its major component was identified as 8-β-D-glucopyranosylgenistein (**1**)[17] which is not commercially available. Hence, synthesis of this glucosylisoflavone is presented here and evaluated for its antidiabetic activity and toxicity.

RESULTS AND DISCUSSION

Chemistry. Preparation of 8-β-D-glucopyranosylgenistein (**1**) started from 2,4-dibenzyloxy-6-hydroxyacetophenone, whose synthesis was successfully accomplished in one single step by dibenzylation of acetophloroglucinol in 69% yield (Scheme 1) as opposed to the four-step procedure previously reported by Kumazawa et al.[22] Its C-glycosylation succeeded in the presence of catalytic $Sc(OTf)_3$ with perbenzylglucosyl acetate. When compared to the previously described conditions based on reaction of the glucosyl fluoride catalyzed by boron trifluoride etherate,[22] our methodology resulted in a reproducible, less expensive, and cleaner reaction, giving compound **8** through a Fries-type rearrangement in reasonable yield (49%). In the alternative, access to **8** succeeded by C-glucosylation of acetophloroglucinol with perbenzylglucosyl acetate catalyzed by TMSOTf in 56% yield, followed by benzylation. Reaction of **8** with 4-benzyloxybenzaldehyde in aqueous NaOH 50% (w/v) followed by acetylation afforded chalcone **9** in 60% overall yield. These conditions have proven reproducible, while those previously reported, based on NaOMe in MeOH solution, did not result in the expected yield.[23]

The oxidative rearrangement of **9** with thallium(III) nitrate (TTN) was performed in basic conditions with aqueous solution of NaOH 50%, leading to the glucosylisoflavone **10** in 63% isolated yield. Debenzylation by catalytic hydrogenation with Pd/C gave 8-β-D-glucopyranosylgenistein (**1**) in 96% yield.

Biological Evaluation. *Effect of 8-β-D-Glucopyranosylgenistein (1) Treatment on Diabetic Animals.* Compound **1** showed an extensive therapeutical impact on an animal model of diabetes characterized by β-cell failure, in which the streptozotocin (STZ) induced diabetic Wistar rats were treated with intraperitoneal (ip) injections of **1** (4 (mg/kg bw)/day) for 7 days. Normalization of fasting hyperglycemia and a major amelioration of excessive postprandial glucose excursions to values close to those observed on healthy normal rats were found, as assessed by an intragastric glucose tolerance test (Figure 1). When compared to the known polyphenols that

Scheme 1. Synthesis of 8-β-D-Glucopyranosylgenistein (1)[a]

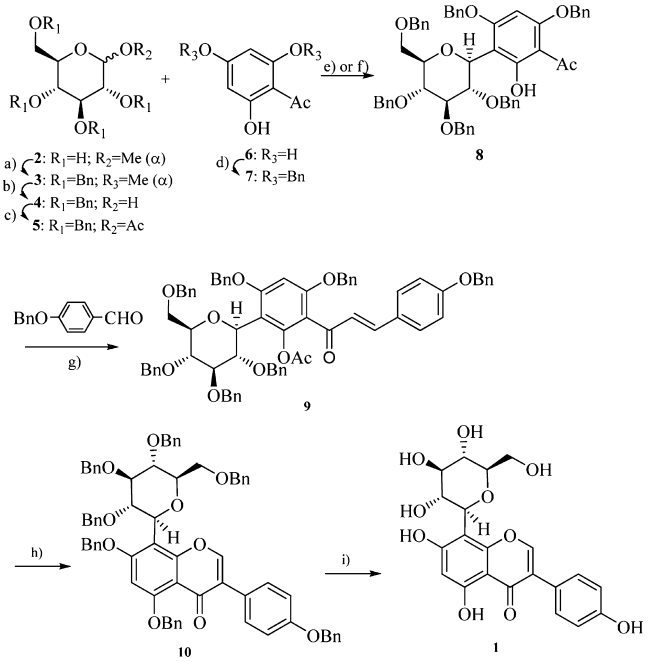

[a](a) (1) NaH, DMF, 0 °C, 30 min; (2) BnBr, rt, 24 h, 87%; (b) AcOH, H_2SO_4 1 M, 90−95 °C, 24 h, 81%; (c) Ac_2O, Py, rt, 1 h, 96%; (d) (1) K_2CO_3, DMF, 0 °C, 30 min; (2) BnBr, rt, 1 h, 69%; (e) R_2 = Ac, R_3 = Bn, $Sc(OTf)_3$, DCE, Drierite, −30 °C, 30 min, then rt, 5 h, 49%; (f) $R_2 = R_3 = H$; (1) TMSOTf, CH_2Cl_2−CH_3CN (1:1), Drierite, −40 °C, 30 min, then rt, 3 h, 56%; (2) K_2CO_3, DMF, 0 °C, 30 min, then BnBr, rt, 1 h, 74%; (g) (1) 1,4-dioxane, aq NaOH 50% (w/v), 18 h, reflux; (2) Ac_2O, Py, DMAP, 1 h, rt, 60%; (h) (1) TTN(III), $(MeO)_3CH$, MeOH, 24 h, 40 °C; (2) THF, MeOH, aq NaOH 50% (w/v), 4 h, rt, 63%; (i) MeOH, EtOAc, Pd/C, H_2, 6 h, rt, 96%.

inhibit IAPP fibrillization, namely, EGCG and PGG, compound **1** is a far more promising candidate. Indeed, a dosage of 100 (mg/kg bw)/day of EGCG for 2 weeks could only slightly improve oral glucose tolerance in high-fat-induced diabetic mice.[11] However, at concentrations of 60−90 (mg/kg bw)/day, this compound was capable of reducing the risk of type I diabetes, which results from the autoimmune-mediated destruction of pancreatic β-cells and deficient insulin production.[12] Additionally, PGG lowered blood glucose level of high-fat-diet-induced diabetic mice only at a dose of 50 (mg/kg bw)/day and after 21 days of treatment.[13] On the seventh day with the same dose only 50% reduction of diabetic mice blood glucose levels were reached, corresponding to 37% increased circulating glucose when compared to the normal control, in contrast to the complete normalization achieved by compound **1** at a dose of 4 (mg/kg bw)/day.

Treatment with compound **1** also increased glucose-induced insulin secretion as estimated through C-peptide insulin parameters, an effect also reported for EGCG.[11] Also, circulating insulin was enhanced (Figures S1 and S2 in Supporting Information) when compared to the values observed after administration of STZ resulting from pancreatic β-cells destruction. Hence, β-cell sensitivity was clearly ameliorated by compound administration (Figure S3).

ThT Fluorescence and AFM Monitoring of IAPP Fibril Formation in the Presence 8-β-D-Glucopyranosylgenistein (1). Rat IAPP amino acid sequence differs from that of humans by the substitution of proline residues in the amyloidogenic

dx.doi.org/10.1021/jm501069h | J. Med. Chem. XXXX, XXX, XXX−XXX

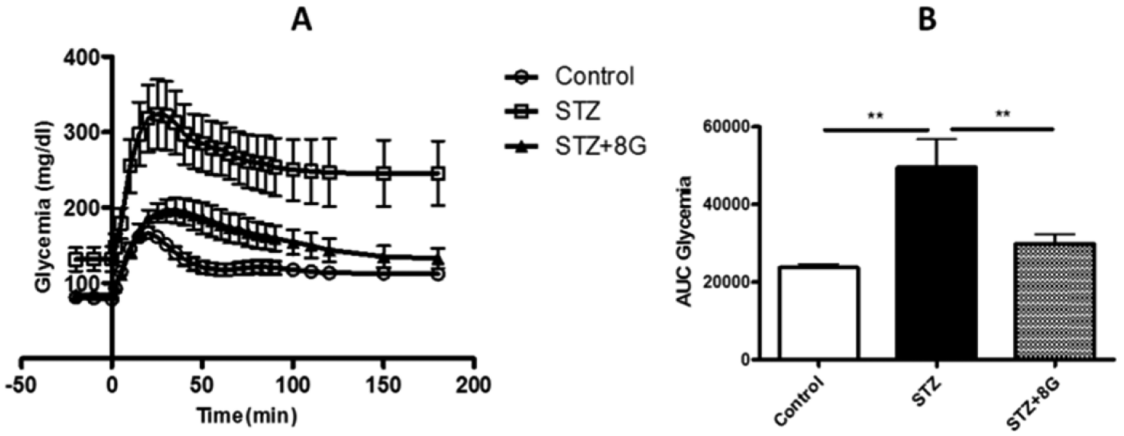

Figure 1. (A) Glycemic curves showing basal fasting and postload (2 mg glucose/kg) values for intragastric glucose tolerance test. (B) Area under the curve (AUC) for the glycemic curves for all groups. 8G = 8-β-D-glucopyranosylgenistein. (**) Differences were considered statistically significant when $p < 0.05$.

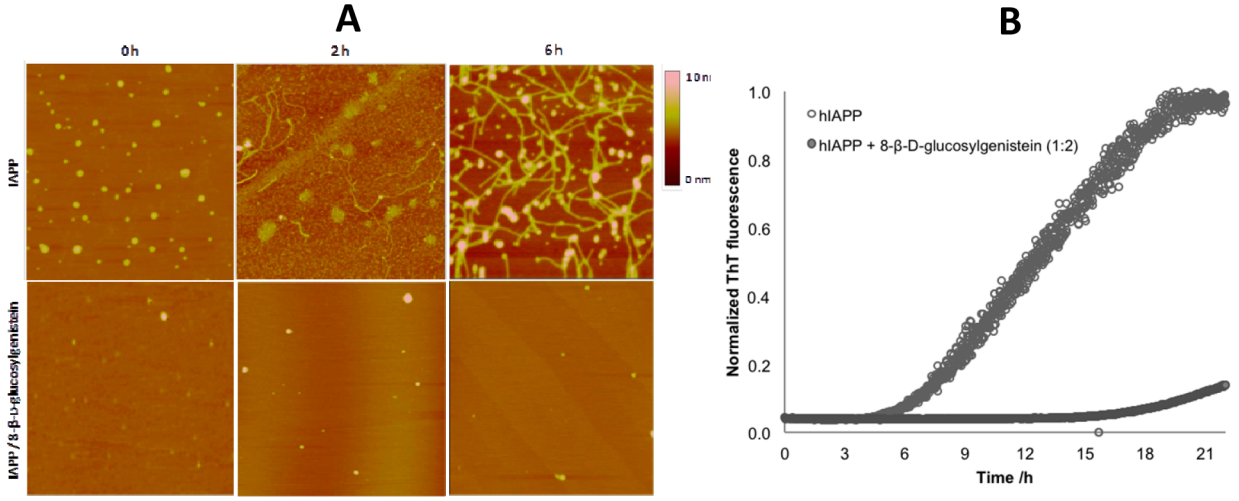

Figure 2. (A) Effect of **1** on IAPP fibrillization, monitored by AFM (z = 10 nm): (top row) control, IAPP (25 μM) incubated for 0, 2, and 6 h at 37 °C without **1**; (bottom row) IAPP (25 μM) incubated for 0, 2, and 6 h at 37 °C, in the presence of compound **1** (50 μM). (B) Inhibition of hIAPP amyloid formation by 8-β-D-glucopyranosylgenistein (**1**), monitored by ThT fluorescence intensity. Thioflavin-T monitored kinetic experiments of hIAPP are shown in the absence (full circles) or presence of 8-β-D-glucopyranosylgenistein (open circles). Arrows indicate the times at which the AFM images were acquired (0, 2, and 6 h).

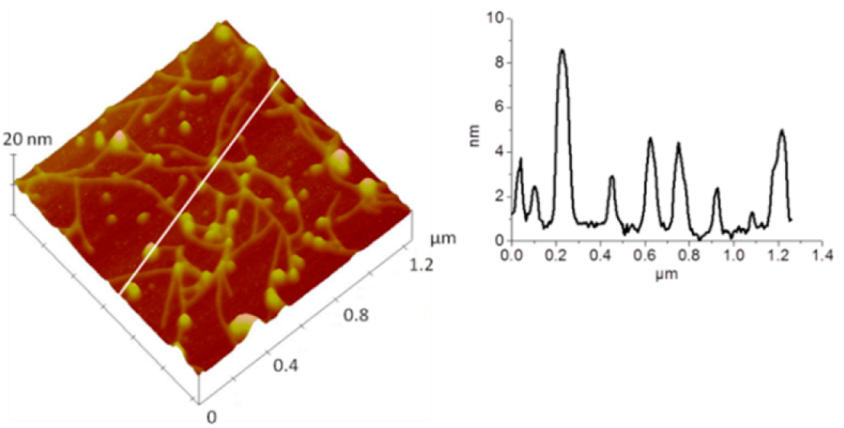

Figure 3. Section analysis of the fibrils and spherical aggregates observed in the control sample, by AFM.

region of the peptide.[24] As a result, it does not form amyloid fibrils or is toxic to β-cells, meaning that, interestingly, compound **1** exerts its antidiabetic effect in rats by a mechanism that does not relate to the inhibition of IAPP amyloid aggregation. Still, considering that EGCG and PGG are known to possess this ability, we were interested in

dx.doi.org/10.1021/jm501069h | J. Med. Chem. XXXX, XXX, XXX–XXX

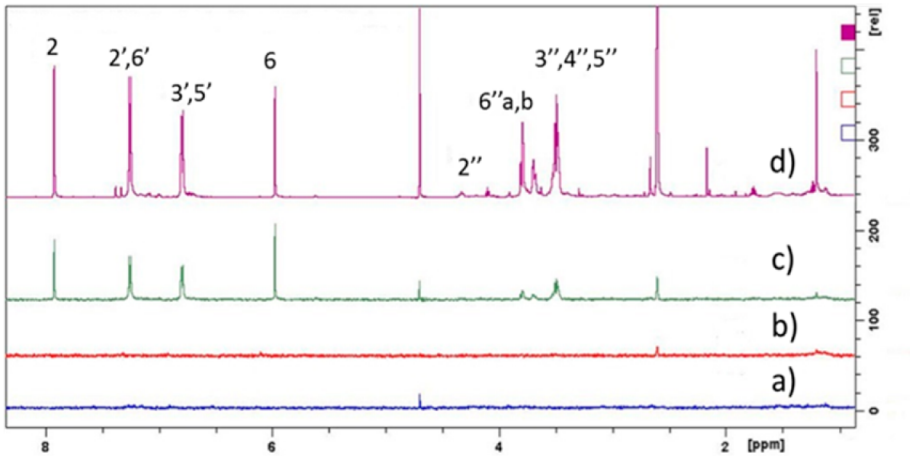

Figure 4. STD result for the 8-β-D-glucopyranosylgenistein (**1**)/IAPP mixture at 298 K along with the corresponding controls. The STD of the IAPP oligomers at the irradiation point (δ −0.5 ppm) (a) was performed to discard the presence of any contaminant, which could interfere in the STD spectrum. The STD of IAPP alone appears completely clean (a). No NMR signals were detected in the STD control of the compound **1** at the same irradiation point (b). The STD experiment was performed on the 8-β-D-glucopyranosylgenistein/IAPP system with 25:1 molar ratio under identical experimental conditions (c). Clear STD signals of 8-β-D-glucopyranosylgenistein (**1**) appeared on the spectrum (c, d).

investigating whether 8-β-D-glucopyranosylgenistein (**1**) can indeed act as an antidiabetic in humans by a multitarget mechanism of action, including the prevention of IAPP amyloid oligomerization. Thus, the binding of compound **1** to IAPP oligomers was investigated.

Inhibition of IAPP fibril formation by **1** at a ratio of 1:2 (hIAPP/**1**) was assessed using atomic force microscopy (AFM) and fluorescence of thioflavin T. The fluorescence results show that at time zero there are no fibrils present, and after a lag phase fibrils start to form (Figure 2B). As a negative control, rat IAPP, which is known not to form fibrils, was used to confirm that the protocol and experimental results are being correctly interpreted, and indeed no changes in ThT fluorescence were detected along the course of the entire experiment (Supporting Information, Figure S4). Human IAPP predominantly aggregates into fibrils with discrete heights of 2−3 nm, although spherical species with heights ranging from 3 to 9 nm are also formed in the absence of compound **1** (Figures 2 and 3). These latter species, commonly referred as oligomers, have been proposed to act as intermediates for fibril formation.[25] We have also detected the presence of some elongated fibrils after 2 h that turned into complex multiple fibrils within 6 h. This is consistent with the time dependence of ThT fluorescence, which shows that, for this sample, large fibrils started to form at ∼5 h. Conversely, after incubation of the peptide with **1** for 6 h, IAPP fibrils were not detected (Figure 2), and again AFM and ThT fluorescence results were consistent. Although a minor amount of spherical aggregates were still observed, their apparent density was significantly reduced when compared to that imaged without compound **1** (control). Already at the initial stages, the addition of **1** resulted in the decrease of the oligomers' density prior to fibril formation. These studies suggest that the binding of **1** results in the inhibition of IAPP amyloid formation, even in their earlier stages. These oligomers, as mentioned above, are thought to be the most toxic type of aggregates.

NMR Binding Experiments with Aβ_{1-42} Oligomers and hIAPP. Recent studies have pointed out multiple lines of evidence linking the incidence of diabetes to the development of Alzheimer's disease.[26] While type 2 DM is associated with IAPP deposits, the accumulation of β-amyloid (Aβ) fibrils is a hallmark of AD. We then investigated the interaction of **1** with amyloid oligomers. The molecular recognition studies of compound **1** with IAPP and Aβ_{1-42} oligomers were conducted employing saturation transfer difference (STD) NMR, a robust method to detect the binding of ligands to a given receptor.[27] Indeed, binding of chemically different molecules to Aβ_{1-42} oligomers has been characterized by STD.[27a] The proper oligomeric state of IAPP and Aβ_{1-42} peptides to be employed for STD experiments was generated using previously reported conditions (see Supporting Information).[28] Figure 4 shows the STD for the 8-β-D-glucopyranosylgenistein/IAPP mixture along with the corresponding controls, which appeared completely clean (Figure 4a and Figure 4b). The STD experiment was then performed on the 8-β-D-glucopyranosylgenistein/IAPP system under identical experimental conditions (Figure 4c). Clear STD signals of compound **1** appeared on the spectrum, in the presence of IAPP (Figure 4c and Figure 4d) or Aβ_{1-42} (Figure S5) oligomers. These results showed, in a nonambiguous way, that **1** interacts with both amyloid peptides.

Analysis of the STD signals obtained for **1** allowed determination of its binding epitope in the presence of IAPP or Aβ_{1-42} peptide oligomers (Figure 5). STD intensities (Figure 5) clearly indicated that the aromatic aglycone is involved in the binding. Nevertheless, several sugar resonances appeared, suggesting their participation in the molecular recognition process. The deduced epitope is the same for both amyloid peptides, indicating the same binding mode for both amyloid aggregates. For comparison reasons also recorded was a STD experiment of the genistein itself in the presence of Aβ_{1-42} peptide oligomers under identical experimental conditions of its glycosylated analog. Interestingly, the epitope map of the genistein (Figure S6) is rather distinct when glycosylated or not. Without the sugar all protons of the aromatic molecule, genistein, receive now almost the same percentage of saturation indicating that no particular proton is in closest contact with the Aβ_{1-42} receptor. This result points out that the introduction of glucose residue on genistein structure induces a preferential binding mode of the aromatic genistein to the Aβ_{1-42} oligomers.

In order to identify the bound conformation of **1** to the amyloid oligomers, trNOESY experiments[29] were carried out.

dx.doi.org/10.1021/jm501069h | J. Med. Chem. XXXX, XXX, XXX−XXX

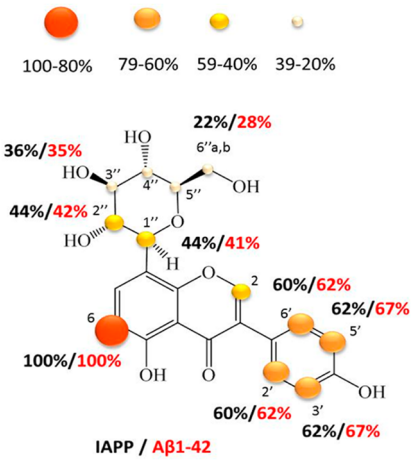

Figure 5. Epitope mapping obtained for 8-β-D-glucopyranosylgenistein (**1**) with IAPP (black labels) and Aβ_{1-42} (red labels) peptide oligomers. The atom numbering used in the NMR analysis is displayed.

The NOESY spectrum of the free compound was first recorded in the absence of amyloid oligomers as control (Figure 6a), yielding positive NOE cross peaks. In contrast, strong and negative NOEs were detected in the presence of Aβ_{1-42} (Figure 6b). This fact reflects an increase of the effective rotational motion correlation time of the molecule in the presence of the Aβ oligomers, further supporting the existence of binding process of **1** to a large molecular entity,[30] here represented by the peptide oligomeric state. The orientation of the glucosyl group with respect to the oligomer was deduced from inspection of the trNOESY cross peaks of compound **1** in the presence of Aβ_{1-42}. Indeed, the trNOESY recorded at 310 K (Figure 6b) showed a cross peak between H2 of the aglycone and H1″ (also H3″ and H5″, mediated by spin diffusion). This cross peak was absent in the NOESY spectrum of the ligand in the free state (Figure 6a). The existence of this cross peak suggests that in the bound state the glucosyl group adopts a preferential conformation whose α-face points toward H2 at the fused bicyclic moiety of the aglycone. In contrast, the absence of NOEs between the glucose and aglycone moiety for **1** in solution suggests a conformational equilibrium of different conformers, where no conformation is defined as the major conformer in solution.

Insights on the geometry of these conformers were obtained by using molecular mechanics (MM) calculations, with the MM3* force field.[30,31] Two conformations around the C1″−C8 linkage were identified, which only differed in 2.6 kJ/mol. The energy barrier for their interconversion was estimated in only 9 kcal/mol, supporting their simultaneous presence in free solution (see above). The global minimum (defined by an antigeometry for the H1″−C1″−C8−C7 torsion angle) is shown in violet in Figure 7, while the alternative local minimum (with a *syn*-orientation) is displayed in yellow.

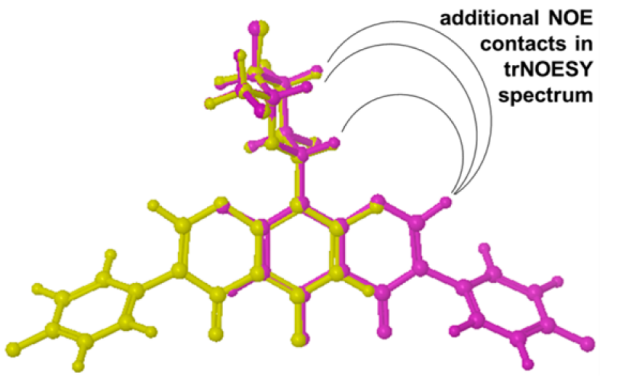

Figure 7. Two conformations around the C1″−C8 linkage of **1**. The global minimum is shown in violet, while the local minimum is in yellow. trNOE experimental contacts are highlighted showing that 8-β-D-glucopyranosylgenistein (**1**) adopts the global minimum conformation in the presence of Aβ_{1-42} oligomers.

According to the trNOESY results, compound **1** preferentially adopts the *anti*-orientation (structure in violet at Figure 7) in the presence of Aβ_{1-42} oligomers. In contrast, it could be assumed that both conformers (*anti* and *syn*) coexist in solution.

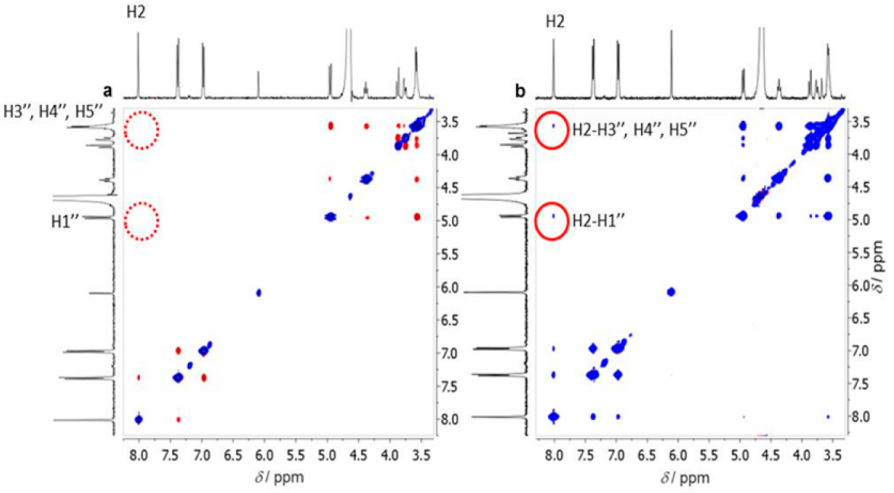

Figure 6. (a) 400 MHz 2D-NOESY spectra of **1** (2 mM) with a mixing time of 0.8 s. (b) trNOESY of the mixture containing Aβ_{1-42} (80 μM) and **1** (2 mM), with a mixing time of 0.3 s. Both samples were dissolved in deuterated PBS, at pH 7.5 and 310 K. Positive cross peaks are in red, and negative ones are in blue.

dx.doi.org/10.1021/jm501069h | J. Med. Chem. XXXX, XXX, XXX−XXX

The sugar moiety is acknowledged to improve bioavailability (e.g., by increasing water solubility) and targeting as well as promoting blood−brain barrier (BBB) crossing.[32,33] Thus, given the structural features of glucosyl isoflavone (**1**), this compound has potential to combine the biocompatible properties of sugars and the well-known ability of polyphenols to inhibit amyloid fibril formation by specific aromatic interactions. Although genistein demonstrated fibril-destabilizing effects and the ability to prevent Aβ oligomerization,[6] the presence of the sugar moiety in compound **1** seems to be a crucial structural feature for the complete aggregate suppression. A recent study showed that several polyphenol glycosides are capable of dissociating Aβ oligomers into nontoxic soluble peptides, in contrast to the respective aglycones, which convert them into large off-pathway aggregates.[34] Hence, this C−C linked glucosylgenistein, which is not chemically or enzymatically cleaved in vivo, is expected to play a similar role. In fact, the STD experiments here presented demonstrated that the presence of the sugar is able to tune the binding mode of the interaction of genistein to the Aβ receptors. This seems to occur in a synergistic combination of the aglycone and the sugar moiety, where the aglycone initiates the remodeling process by disrupting intermolecular contacts between Aβ peptide through π-stacking interaction, whereas CH−π stacking interactions driven by association of the CH sugar bonds with π-electron cloud of the aromatic rings were suggested to cause interaction of sugars with the newly exposed aromatic rings, ultimately preventing Aβ residues from associating between them. Both this study and our STD experimental results give insights into the advantages of compound **1** when compared to genistein in the suppression of amyloid fibril formation.

The acute toxicity of **1** in eukaryotic cells was assessed by the MTT cell viability assay. Compound **1** exhibited an IC_{50} value of 1.25 mg/mL, almost 10 times higher than that of the commercial drug chloramphenicol (0.143 mg/mL). The potential genotoxic activity of **1** was also evaluated by scoring chromosomal aberrations on metaphase spread, and no evidence for genotoxic risk was found.[21]

CONCLUSION

8-β-D-Glucopyranosylgenistein (**1**) has been successfully accessed by synthesis, produces normalization of fasting hyperglycemia in STZ induced diabetic Wistar rats, and interferes in glucose excursions increasing glucose-induced insulin secretion and insulin sensitivity. This nontoxic glucosylflavonoid is the most potent antidiabetic molecular entity described so far that interacts with both toxic $A\beta_{1-42}$ and IAPP amyloid oligomers, preventing amyloid fibrillization characteristic of diabetic patients. These properties encourage its further exploitation toward innovative therapeutics to circumvent the tendency of diabetic patients to develop AD. Its use as a functional food ingredient will provide specific health benefits for the prevention of functional and cognitive decline, a major issue to succeed in promoting a healthy life and an active aging.

EXPERIMENTAL SECTION

Chemistry. Reagents and solvents were purchased from Sigma-Aldrich (Barcelona, Spain). All nonaqueous reactions were carried out under an atmosphere of N_2 using freshly distilled and dry solvents, unless otherwise noted. Reactions were monitored by thin layer chromatography (TLC), which was carried out on 0.25 mm silica gel F_{254} plates (Merck, Germany) using UV light, a 5% ethanol solution of ferric chloride, and a 10% sulfuric acid in ethanol, followed by heating at 120 °C, as visualization agents. Silica gel 60G (0,040−0,063 mm) from Merck (Germany) was used for column chromatography (CC). Nuclear magnetic resonance (NMR) spectra were recorded at room temperature (rt), on a Bruker Advance 400 apparatus, using tetramethylsilane (TMS) as an internal standard. Chemical shifts δ are given in ppm, and NMR data are in full agreement with that given in the literature.[22,23] Purity of all compounds, >95%, was detected by high resolution mass spectra, acquired on a Bruker Daltonics APEX Ultra FT-ICR mass spectrometer (Billerica, MA, USA) equipped with a 7.0 T actively shielded superconducting magnet from Magnex Scientific. The ions were generated from an external Apollo II dual ESI/MALDI source from Bruker Daltonics. Samples were introduced by means of an infusion pump at a flow rate of 120 μL/h. The nebulizer gas (N_2) flow rate was set to 2.5 L/min, and the drying gas (N_2) flow rate was set to 4.0 L/min at a temperature of 220 °C. The capillary voltage was set to 4100 V and the spray shield voltage was set to 3700 V.

2,4-Dibenzyloxy-6-hydroxyacetophenone (7). To a solution of acetophloroglucinol **6** (10.02 g, 59.6 mmol) in DMF was added K_2CO_3 (2.2. equiv). After stirring for 10 min at 0 °C, BnBr (2.2. equiv) was added and the mixture stirred for 1 h. HCl, 2 M, was added, and the mixture was poured into water and extracted with EtOAc. Organic layers were combined, washed with brine, dried over $MgSO_4$, and concentrated. Compound **7** was purified by CC (10:1 hexane/EtOAc) in 69% yield (14.32 g, 41.12 mmol). R_f = 0.73 (4:1 petroleum ether/EtOAc); mp 103.5−104.0 °C (lit. mp 108−109 °C);[22] ^{1}H NMR ($CDCl_3$) δ = 14.22 (s, 1H; OH-8), 7.47−7.40 (m, 10H, C*H*-Ph), 6.22 (d, ^3J(5,7) = 2.3 Hz, 1H; H-7), 6.15 (d, ^3J(5,7) = 2.3 Hz, 1H; H-5), 5.09 (s, 2H; CH_2Ph-4), 5.08 (s, 2H; CH_2Ph-6), 2.61 (s, 3H; H-1); ^{13}C NMR ($CDCl_3$) δ 203.2 (C-2); 167.6 (C-6, C-8); 162.1 (C-4); 135.9 (C_q-4); 135.7 (C_q-6); 128.8, 128.8, 128.5, 128.4, 128.1, 127.7 (CH, Ph); 106.3 (C-3); 94.8 (C-7); 92.4 (C-5); 71.2 (CH_2Ph-6); 70.3 (CH_2Ph-4); 33.4 (C-1). HRMS: calcd for [M + Na] 371.1254; found 371.1257.

2,4-Dibenzyloxy-6-hydroxy-5-(2,3,4,6-tetra-*O*-benzyl-β-D-glucopyranosyl)acetophenone (8). *Method A.* 1-*O*-Acetyl-2,3,4,6-tetra-*O*-benzyl-α-D-glucopyranose (**5**, 1.28 g, 2.20 mmol) and **7** (2.0 equiv) were dissolved in DCE (10 mL) in the presence of Drierite (100 mg). The solution was stirred at −30 °C, and $Sc(OTf)_3$ (0.25 equiv) was added. The stirring continued for 30 min at −30 °C and then at room temperature for 5 h. The reaction was quenched with water and filtered through Celite, extracted with DCM, and concentrated. Compound **8** was purified by CC (10:1 petroleum ether/EtOAc) and isolated in 49% yield as a syrup (0.94 g, 1.08 mmol).

Method B. To a solution of acetophenone (**6**, 5.96 mmol, 2.0 equiv) dissolved in ACN (25 mL) was added a solution of compound **4** (1.61 g, 2.98 mmol) in DCM (25 mL). Drierite (100 mg) was added, and the reaction was kept at −40 °C under N_2 atmosphere. TMSOTf (0.5 equiv) was added to the reaction, and the cooling bath was kept for 30 min. The bath was removed and reaction reached room rt and was run for 3 h. The reaction was quenched with $NaHCO_3$, extracted with DCM, washed with brine, dried over $MgSO_4$, and concentrated in vacuum. The desired product was purified by CC (7:1 hexane/ethyl acetate) and isolated in 56% yield (1.15 g, 1.67 mmol). R_f = 0.21 (2:1 hexane/EtOAc); ^{1}H NMR ($CDCl_3$) δ = 7.34−6.98 (m, 20H; C*H*-Ph), 5.89 (*s*, 1H; H-7), 4.88 (d, 1H, $J_{1',2'}$ = 9.71 Hz, H-1′); 4.97−4.48 (m, 8H; CH_2Ph), 3.81−3.60 (m, 6H; H-2′, H-3′, H-4′, H-5′, H-6a′, H-6b′), 2.56 (*s*, 3H; H-1); ^{13}C NMR ($CDCl_3$) δ = 203.9 (C-2); 164.0 (C-6); 161.9 (C-4); 161.4 (C-8); 138.3, 137.7, 137.0, 136.6 (C_q, Ph); 128.6, 128.5, 128.3, 128.1, 127.7, 127.6 (CH, Ph); 105.7 (C-5); 102.4(C-3); 97.1 (C-7); 86.2 (C-2′); 81.7 (C-3′); 78.7 (C-4′); 77.4 (C-5′); 75.7 (C-1′); 75.9, 75.2, 74.8, 74.5 (CH_2Ph); 68.1 (C-6′); 32.9 (C-1). HRMS: calcd for [M + Na] 713.2721; found 713.2735.

This *C*-glucosyl derivative was dissolved in DMF (23 mL). To this solution K_2CO_3 (2.2 equiv) was added at 0 °C and stirred for 10 min at 0 °C. Then BnBr (2.2 equiv) was added and the reaction was allowed to reach rt and run for 2 h. After completion, the reaction was neutralized with HCl, 2M, extracted with DCM, washed with brine,

dried over $MgSO_4$, and concentrated. The product was isolated by CC (6:1 hexane/EtOAc) in 74% yield (1.08 g, 1.24 mmol). R_f = 0.33 (4:1 petroleum ether/EtOAc); ^{1}H NMR ($CDCl_3$) δ = 14.11(s, 1H; OH-4), 7.43−6.89 (m, 30H; C*H*-Ph), 6.36 (*s*, 1H; H-7), 4.96−4.45 (m, 13H; CH_2Ph, H-1′), 3.74−3.37 (m, 6H; H-2′, H-3′, H-4′, H-5′, H-6a′, H-6b′), 2.52 (*s*, 3H; H-1); ^{13}C NMR ($CDCl_3$) δ = 203.1 (C-2); 164.7 (C-4); 163.5 (C-6); 160.7 (C-8); 138.7, 138.6, 138.2, 138.1, 137.9, 137.4, 137.5, 136.4, 135.8; (C_q. Ph); 128.5, 128.5, 128.4, 128.3, 128.2, 128.1, 128.0, 128.0, 127.9, 127.8, 127.7, 127.6, 127.6, 127.6, 127.3, 126.2 (*C*H. Ph); 111.5 (C-5); 105.9 (C-3); 90.0 (C-7); 82.1 (C-3′); 78.8 (C-5′); 77.6 (C-4′); 77.4, 77.1, 76.7, 75.7, 75.7, 75.7, 75.3, 75.3, 75.0, 73.5, 73.4, 73.2 (*C*H$_2$Ph); 72.8 (C-2′); 70.0 (C-1′); 68.4 (C-6′); 33.5(C-1). HRMS: calcd for [M + Na] 893.3660; found 893.3694.

(2*E*)-1-[2-Acetoxy-4,6-dibenzyloxy-3-(2,3,4,6-tetra-*O*-benzyl-*β*-D-glucopyranosyl)]phenyl-3-(4-benzyloxyphenyl)pro-2-en-1-one (9). To a solution of **8** (2.44 g, 2.80 mmol) and *p*-benzyloxybenzaldehyde (1.5 equiv) in 1,4-dioxane (27.9 mL) was added an aqueous solution of NaOH 50% (27.9 mL). The reaction mixture was stirred in reflux for 24 h. After this time HCl, 2 M, was added and the mixture was extracted with DCM, washed with brine, dried over $MgSO_4$, and concentrated. The residue was dissolved in pyridine (10 mL/g residue) and acetic anhydride (2.0 equiv/OH). The mixture was stirred for 30 min, and then pyridine was removed. Compound **9** was isolated by CC (5:1 petroleum ether/EtOAc) as a syrup in 60% overall yield (1.86 g, 1.68 mmol). R_f = 0.50 (3:1 petroleum ether/EtOAc); ^{1}H NMR ($CDCl_3$) δ = 7.49−7.21 (m, 38H; CH-Ph, H-3, H-3′, H-5′), 6.96 (d, ^3J(2′,3′) = 8,6 Hz, 1H; H-6′), 6.91 (d, ^3J(2,3) = 16,15 Hz, 1H; H-2), 6.43 (s, 1H; H-5′), 5.14 (s, 2H, CH_2Ph-7), 5.04−4.14 (m, 4H; CH_2Ph, H-1‴, H-2‴), 3.91−3.48 (m, 5H; H-3‴, H-4‴, H-5‴; H-6a‴, H-6b‴); 2.09 (s, 3H; OCH_3-Ac); ^{13}C NMR ($CDCl_3$) δ = 191.9 (C-1); 169.4 (CO-Ac); 160.7 (C-6′); 159.6 (C-1′, C-4′); 157.5 (C-4″); 149.5 (C-2″); 144.8 (C-3); 138.9, 138.8, 138.6, 138.1, 136.7, 136.6 (Cq, Ph); 136.2 (Cq, Ph-7); 128.8, 128.7, 128.6, 128.5, 128.4, 128.3, 128.2, 128.1, 128.0, 127.9, 127.8, 127.7, 127.6, 127.5, 127.4, 127.3, 127.2(CH, Ph); 127.1 (C-3′, C-5′); 126.3 (C-2); 118.9 (C-1″); 115.3 (C-2′, C-6′); 113.4 (C-3″); 96.7 (C-5″); 87.3 (C-3‴); 81.5 (C-2‴); 79.4 (C-5‴); 78.1 (C-4‴); 75.2; 74.9; 74.2; 73.1; 71.4; 70.8; 70.2 (CH_2Ph); 73.7 (C-1‴); 69.7 (CH_2Ph-7); 69.2 (C-6‴); 29.9 (OCH_3). HRMS: calcd for [M + Na] 1129.4497; found 1129.4512.

4′,5,7-Tri-*O*-benzyl-8-(2,3,4,6-tetra-*O*-benzyl-*β*-D-glucopyranosyl)genistein (10). TTN (2.0 equiv) was added to a solution of **9** (1.85 g, 1.67 mmol) in $(MeO)_3CH$ (45 mL) and MeOH (45 mL). The reaction mixture stirred for 24 h at 40 °C and then sodium bissulfite was added to promote the reduction of Tl(III) to Tl(I). Solid was removed by filtration. Water was added, and the mixture was extracted with DCM. The combined extracts were dried over $MgSO_4$, filtered off, and concentrated. The yellow residue was dissolved in THF (21 mL) and MeOH (21 mL), and then aqueous NaOH 50% (8.6 mL) was added and the reaction stirred for 4 h at room temperature. After reaction completed, HCl, 2 M, was added and the mixture was extracted with DCM, dried over $MgSO_4$, filtered off, and concentrated. The residue was separated by CC (petroleum ether/EtOAc, 5:1) to give **10** as a syrup in 63% overall yield (1.12g, 1.05 mmol). R_f = 0.45 (petroleum ether/EtOAc, 3:1); ^{1}H NMR ($CDCl_3$) δ = 7.77 (s, 1H; H-2), 7.60−6.95 (m, 35H; C*H*-Ph), 6.84 (d, ^3J(2′,3′) = J(5′,6′) = 7.2 Hz, 2H; H-2′, H-6′), 6.75 (d, 2H; H-3′, H-5′), 6.40 (s, 1H; H-6)*; 5.25−4.05 (m, 14H; CH_2Ph, H-1″); 3.95−3.53 (m, 6H; H-2″, H-3″, H-4″, H-5″, H-6a″, H-6b″); ^{13}C NMR ($CDCl_3$) δ = 180.9 (C-4), 163.2 (C-7), 163.0 (C-5), 155.9 (C-8a), 152.5 (C-2), 138.7, 138.6, 138.5, 138.3, 138.2, 137.8, 137.1 (C_q, Ph), 129.9, 130.1 (C-2′, C-6′); 128.7, 128.6, 128.5, 128.4, 128.3, 128.2, 128, 1, 128.0, 127.9, 127.8, 127.6, 127.5, 127.3, 127.2, 127.1 (*C*H, Ph), 115.0, 115.1 (C-3′, C-5′),123.0 (C-3), 122.9 (C-1′), 106.4 (C-4a), 104.8 (C-8), 96.6 (C-6), 87.9 (C-2″), 79.6 (C-5″), 78.5 (C-4″), 75.9, 75.6, 75.2, 74.8, 74.2, 73.5, 73.2 (*C*H$_2$Ph), 74.5 (C-3″), 68.9 (C-6″). *Duplication of the peaks was observed, corresponding to rotamers. HRMS: calcd for [M + H] 1063.4416; found 1063.4465.

8-*β*-D-Glucopyranosylgenistein (1). Pd/C (25 mg) was added to a solution of **10** (0.1 g, 0.094 mmol) in MeOH (3 mL) and EtOAc (1 mL), which was stirred at room temperature for 2 h under hydrogen atmosphere. Catalyst was filtered off under Celite and washed with MeOH. The filtrate was concentrated and purified by CC (6:1 petroleum ether/EtOAc) to give compound **1** as a syrup in 96% yield (0.039g, 0.09 mmol). R_f = 0.35 (1:1 petroleum ether/EtOAc); ^{1}H NMR (acetone-d_6) δ = 13.05 (s, 1H; OH-5), 8.06 (s, 1H; H-2), 7.31 (d, ^3J(2′,3′) = 8.9 Hz, 2H; H-2′, H-6′), 6.76 (d, 2H; H-3′, H-5′), 6.12 (s, 1H; H-6), 4.91 (d, ^3J(1″,2″) = 9.9 Hz, 1H; H-1″), 3.74−3.70 (m, 3H; H-2″, H-6a″, H-6b″); 3.56 (t, ^3J(2′,3′)=9.93 Hz, 1H; H-4″); 3.48 (*t*, 1H, ^3J(2″,3″) = 9.9 Hz, H-3″); 3.38 (td, ^3J(5″,6a″) = ^3J(5″,6b″) = 2.9 Hz, 1H; H-5″); ^{13}C NMR (acetone-d_6) δ 182.1 (C-4); 164.0 (C-5); 163.3 (C-7); 158.5 (C-4′); 156.7 (C-8a);154.4 (C-2); 131.3 (C-2′, C-6′); 123.8 (C-3); 123.0 (C-1′); 116.2 (C-3′, C-5′); 106.1 (C-4a); 104.1 (C-8); 100.8 (C-6); 82.1 (C-5″); 79.4 (C-3″); 75.8 (C-1″); 73.7 (C-2″); 70.9 (C-4″); 61.9 (C-6″). HRMS: calcd for [M + H] 433.1129; found 433.1132.

Biological Studies. *Animals.* Tests were conducted using male Wistar rats, with an average weight of 250 g. Animals were maintained under stable conditions of temperature (25 °C), light−dark periods (12 h), and feeding (maintenance rat chow). Both food and water were available ad libitum. Food was removed 24 h before testing to ensure that animals were on the fasting state. Free access to water was maintained during this period. The animals were bred and utilized at the Animal House of the Faculty of Medical Sciences, Lisbon, Portugal. This facility has SPF (specific pathogen free) standards, as supervised by the DGV—Portuguese General Directorate of Veterinary.

Induction of Diabetes. A state of hyperglycemia adequate to the diagnosis of diabetes was induced experimentally through chemical intervention. A sole intraperitoneal (ip) injection of streptozotocin (STZ), previously dissolved in saline, was administered at a dose of 40 mg/kg bw. Hyperglycemia was checked 2 days after STZ administration by quantifying glucose on a blood sample collected by tail puncture. The animals of the normal control group received instead an injection of the same volume of saline, with glycemia checked also after 2 days.

Experimental Animal Groups. Animals were randomly divided into three groups. Group I (control) was given one saline injection, and 2 days after started a 7-day treatment with saline + 5% ethanol. This group represents normoglycemic control. Group II (STZ) was first treated with streptozotocin (40 mg/kg bw, ip) and then for 7 days with saline + 5% ethanol. This group represents the diabetic condition. Group III (STZ + 8G) was first given STZ (40 mg/kg bw, ip) and then a 7-day treatment with synthesized 8-*β*-D-glucopyranosyliso-flavone (**1**, 4 mg/kg/day in saline + 5% ethanol, ip).

Glucose Tolerance Curve and Associated Insulin Parameters. Animals were anesthetized with sodium pentobarbital (65 mg/kg bw) after a 24 h fasting period. Immediately after, they were placed on a homeothermic apparatus. Body temperature was maintained at 37 °C to avoid metabolic changes induced by hypoglycemia. An exterior loop was surgically placed between the femoral vein and artery, and a catheter was placed on the stomach. After surgery completion, recovery before testing was allowed for a minimum period of 30 min. Anesthesia was maintained throughout the experiment with a constant sodium pentobarbital perfusion on the femoral vein. Glucose tolerance testing was done first by monitoring blood glycemia at the fasting state for 20 min, after which 2 mL of a glucose solution (2 mg glucose/kg bw) was administered through the gastric catheter directly into the stomach. Blood glycemia was thus measured at regular intervals by a bench glucose analyzer, both on baseline fasting (from −20 to 0 min) and on the postload period (from 0 to 180 min). Blood samples were also collected for insulin and C-peptide quantification, both at baseline and at postload time points (−20, −10, 0, 5, 15, 30, 45, 60, 90, 120, 180 min). These samples were quickly centrifuged, and serum was stored at −80 °C for RIA analysis.

Data Analysis. Data is shown as the mean ± standard error. Mean relates to *n* observations, in which *n* represents the number of animals tested (between five and eight, depending on the group). Mean values between groups were compared using one-way analysis of variance

dx.doi.org/10.1021/jm501069h | J. Med. Chem. XXXX, XXX, XXX−XXX

(ANOVA), followed by a Tukey post-test. Differences were considered statistically significant when $p < 0.05$.

Kinetics of IAPP Fibrillization by ThT Fluorescence and AFM Morphological Studies. hIAPP (human islet amyloid polypeptide, sequence K^1CNTATCATQRLANFLVHSSNNFGAILSSTN-VGSNTY^{37}-NH_2) and rIAPP (rat islet amyloid polypeptide, sequence K^1CNTATCATQRLANFLVRSSNNLGPVLPPTNVGSNTY^{37}-NH_2) were purchased from Peptide 2.0 (Chantilly, USA) as lyophilized powder. 1,1,1,3,3,3-Hexafluoropropan-2-ol (HFIP) and thioflavin T (ThT) were purchased from Sigma-Aldrich (Barcelona, Spain). hIAPP was dissolved in HFIP followed by brief vortexing to mix and dissolve. The stock solution was sealed with Parafilm and stored at 4 °C until required at a concentration of 100 μM. The HFIP treatment maintains the amyloidogenic peptide in a monomeric soluble state and allows for experimental reproducibility.[35] Prior to experimental use, HFIP was evaporated under a gentle N_2 flow, followed by vacuum pump. The residue was then resuspended in phosphate buffer (pH 7.4, 100 mM sodium phosphate, 100 mM NaCl). Each fibril formation reaction was performed at the final concentrations of 25 μM IAPP and 5 μM ThT, with 2% DMSO. Experiments were carried out in the absence (control) and in the presence of 8-β-D-glucopyranosylgenistein (**1**) at the concentration of 50 μM in a 96-well plate in duplicate. Fluorescence was monitored at 25 °C, with excitation at 440 nm and emission at 480 nm, using a SpectraMax Gemini microplate reader with slit width of 5 nm and a cutoff filter at 455 nm and stirring before each reading. The emission intensity was measured over a time course of 22 h until a plateau for the respective intensity levels was reached. As a negative control, rat IAPP, which is known not to form fibrils, was used at a final concentration of 25 μM to confirm that the protocol and experimental results are being correctly interpreted (Figure S4). For the morphological characterization, Nanoscope IIIa multimode atomic force microscope produced by Digital Instruments (Veeco, Santa Barbara, CA) was used. All measurements were carried out by tapping mode AFM using etched silicon tips with a resonance frequency of ~300 kHz at a scan rate of ~1.5 Hz. The images were acquired in ambient conditions (20 °C) by placing a drop of the solution onto freshly cleaved mica for 15 min, rinsing with water and drying with pure N_2. The AFM experiments were performed with aliquots of the same initial sample that was used for ThT fluorescence assays to allow direct comparison of the data.

NMR Binding Studies with Islet Amyloid Peptide IAPP and Aβ_{1-42} Oligomers. NMR experiments were recorded on a Bruker Avance 600 MHz spectrometer equipped with a triple channel cryoprobe head (IAPP) or on a Varian 400 MHz Mercury instrument (Aβ_{1-42}). Immediately before use, lyophilized Aβ_{1-42} and IAPP were dissolved in 10 mM NaOD in D_2O at a concentration of 160 μM, then diluted 1:1 with 10 mM phosphate buffer saline, pH 7.4, containing 100 mM NaCl (PBS). To these samples were added the compound 8-β-D-glucopyranosylgenistein to a final concentration of 2 mM and ~1 mg in the case of ethyl acetate extract of *G. tenera*. The pH of each sample was verified with a microelectrode (Mettler Toledo) for 5 mm NMR tubes and adjusted with NaOD and/or DCl. All pH values were corrected for isotope effect. Selective saturation of the protein resonances (on resonance spectrum) was performed by irradiating at −0.5 ppm (IAPP) or at −1.0 ppm (Aβ_{1-42}) using a series of Gaussian-shaped or Eburp2.1000-shaped pulses (50 ms) for a total saturation time of 2.0 s. For the reference spectrum (off resonance), the samples were irradiated at 100 ppm. At the end, STD experiments were recorded at two temperatures 298 and 310 K with a ligand/amyloid oligomers molar ratio of 25:1. For NOESY and trNOESY experiments the basic Varian and Bruker sequences were employed. The trNOESY analysis is based on the well-known fact that given the appropriate kinetic conditions for the ligand−receptor association process, NOE cross peaks for small ligands, when free in solution, display a different sign (positive cross peaks, opposite signal to the diagonal peaks) than those recorded for their bound states, in the presence of the receptor (negative cross peaks, same signal of diagonal peaks).[27] A mixture of ligand/amyloid oligomers 25:1 was employed to record trNOESY experiments. For the quantitative NMR experiment, 1.5 mg of ethyl acetate extract of *G. tenera* was dissolved in 550 μL of D_2O and DSS was added to the final concentration of 0.4 mM. A ^{1}H spectrum was acquired with a recycle delay of 60 s to achieve the complete relaxation of all the resonances at each scan. The quantification was performed by comparing the DSS methyl resonance integral with the 8-β-D-glucopyranosylgenistein (**1**) aromatic resonance integrals.

Molecular Mechanics (MM) Calculations. Molecular mechanics were conducted with MacroModel 9.6.207[36] as implemented in version 9.1.207 of the Maestro suite,[37] using the MM3* force field.[31,38] A systematic variation of the torsional degrees of freedom of the molecules permitted generation of different starting structures that were further minimized to provide the corresponding local minima. Only the same two minima were always found for each molecule (*O*- and *C*-glucosides). The continuum GB/SA solvent model[39] was employed, and the general PRCG (Polak−Ribiere conjugate gradient) method for energy minimization was used. An extended cutoff was applied.

■ ASSOCIATED CONTENT

Ⓢ Supporting Information

Antidiabetic activity (C-peptide, insulin, and β-cell sensitivity graphs), ThT kinetics of IAPP fibrillization (rIAPP negative control graph; hIAPP and rIAPP sequence), and NMR binding studies with islet amyloid peptide IAPP and Aβ_{1-42} oligomers (STD NMR, 2D-NOESY, and trNOESY supporting data). This material is available free of charge via the Internet at http://pubs.acs.org.

■ AUTHOR INFORMATION

Corresponding Author

*Phone: +351217500952 or +351964408824. E-mail: aprauter@fc.ul.pt.

Author Contributions

The manuscript was written through contributions of all authors. All authors have given approval to the final version of the manuscript.

Notes

The authors declare no competing financial interest.

■ ACKNOWLEDGMENTS

The authors thank Fundação para a Ciência e a Tecnologia (FCT) for financial support of the Projects PTDC/QUI/67165/2006, Pest-OE/QUI/UI0612/2013, and RECI/BBB-BQB/0230/2012, as well as for the Ph.D. grant of Ana M. Matos (Grant SFRH/BD/93170/2013), the postdoctoral grant of Filipa Marcelo (Grant SFRH/BPD/65462/2009), and IF 2012/2013 initiatives (P.O.P.H., F.S.E.). FCT is also acknowledged for the Project REDE/1501/REM/2005, and Dr. Carlos Cordeiro is acknowledged for providing the HRMS spectrum with the FTICR-MS at the Faculdade de Ciências da Universidade de Lisboa, Portugal. The European Commission is acknowledged for the approval of INOVAFUNAGEING Commitment. The European Community's Seventh Framework Programme (FP7/2007−2013) under Grant Agreements 610359 and 212043 is gratefully acknowledged. F.N. and C.A. thank Fondo per la Promozione di Accordi Istituzionali, Progetto No. 4779 "Network Enabled Drug Design (NEDD)" from Lombardia. J.J.-B. thanks MICINN of Spain (Grant CTQ2009-08536) and the Cariplo Foundation for funding.

■ ABBREVIATIONS USED

STZ, streptozotocin; STD, saturation transfer difference; NMR, nuclear magnetic resonance; trNOESY, transferred nuclear Overhauser effect spectrometry; IAPP, islet amyloid polypeptide; ThT, thioflavin T; ATM, atomic force microscopy; Aβ_{1-42},

amyloid β 1−42; bw, body weight; MM, molecular mechanics; DM, diabetes mellitus; AD, Alzheimer's disease; EGCG, (−)-epigallocatechin 3-gallate; PGG, 1,2,3,4,6-penta-*O*-galloyl-β-D-glucopyranose; TTN, thallium(III) nitrate; ip, intraperitoneal; AUC, area under the curve; hIAPP, human islet amyloid polypeptide; rIAPP, rat islet amyloid polypeptide; Aβ, β-amyloid; BBB, blood−brain barrier; TLC, thin layer chromatography; CC, column chromatography; TMS, tetramethylsilane; rt, room temperature; mp, melting point; HFIP, 1,1,1,3,3,3-hexafluoropropan-2-ol

REFERENCES

(1) Chiti, F.; Dobson, C. M. Protein misfolding, functional amyloid, and human disease. *Annu. Rev. Biochem.* **2006**, *75*, 333−366.

(2) Glabe, C. Common mechanisms of amyloid oligomer pathogenesis in degenerative diseases. *Neurobiol. Aging* **2006**, *27*, 570−575.

(3) Meier, J. J.; Kayed, R.; Lin, C.; Gurlo, T.; Haataja, L.; Jayasinghe, S.; Langen, R.; Glabe, C. G.; Butler, P. C. Inhibition of human IAPP fibril formation does not prevent β-cell death: evidence for distinct actions of oligomers and fibrils of human IAPP. *Am. J. Physiol.: Endocrinol. Metab.* **2006**, *291*, 1317−1324.

(4) Baglioni, S.; Casamenti, F.; Bucciantini, M.; Luheshi, L. M.; Taddei, N.; Chiti, F.; Dobson, C. M.; Stefani, M. Prefibrillar amyloid aggregates could be generic toxins in higher organisms. *J. Neurobiol.* **2006**, *26*, 8160−8167.

(5) Ladiwala, A. R.; Dordick, J. S.; Tessier, P. M. Aromatic small molecules remodel toxic soluble oligomers of amyloid β through three independent pathways. *J. Biol. Chem.* **2011**, *286*, 3209−3218.

(6) Hirohata, M.; Ono, K.; Takasaki, J.; Takahashi, R.; Ikeda, T.; Morinaga, A.; Yamada, M. Anti-amyloidogenic effects of soybean isoflavones in vitro: fluorescence spectroscopy demonstrating direct binding to Aβ monomers, oligomers and fibrils. *Biochim. Biophys. Acta* **2012**, *1822*, 1316−1324.

(7) Cao, P.; Raleigh, D. P. Analysis of the inhibition and remodeling of islet amyloid polypeptide amyloid fibers by flavanols. *Biochemistry* **2012**, *51*, 2670−2683.

(8) Meng, F.; Abedini, A.; Plesner, A.; Verchere, C. B.; Raleigh, D. P. The flavanol (−)-epigallocatechin 3-gallate inhibits amyloid formation by islet amyloid polypeptide, disaggregates amyloid fibrils and protects cultured cells against IAPP-induced toxicity. *Biochemistry* **2010**, *49*, 8127−8133.

(9) Fujiwara, H.; Tabuchi, M.; Yamaguchi, T.; Iwasaki, K.; Furukawa, K.; Sekiguchi, K.; Ikarashi, W.; Kudo, Y.; Higuchi, M.; Saido, T. C.; Maeda, S.; Takashima, A.; Hara, M.; Yaegashi, N.; Kase, Y.; Arai, H. A traditional medicinal herb *Paeonia suffruticosa* and its active constituent 1,2,3,4,6-penta-*O*-galloyl-β-D-glucopyranose have potent anti-aggregation effects on Alzheimer's amyloid β proteins in vitro and in vivo. *J. Neurochem.* **2009**, *109*, 1648−1657.

(10) Bruno, E.; Pereira, C.; Roman, K. P.; Takiguchi, M.; Kao, P.; Nogaj, L. A.; Moffet, D. A. IAPP aggregation and cellular toxicity are inhibited by 1,2,3,4,6-penta-*O*-galloyl-β-D-glucose. *Amyloid* **2013**, *20*, 34−38.

(11) Wolfram, S.; Raederstorff, D.; Preller, M.; Wang, Y.; Teixeira, S. R.; Riegger, C.; Weber, P. Epigallocatechin gallate supplementation alleviates diabetes in rodents. *J. Nutr.* **2006**, *136*, 2512−2518.

(12) Fu, Z.; Zhen, W.; Yuskavage, J.; Liu, D. Epigallocatechin gallate delays the onset of type 1 diabetes in spontaneous non-obese diabetic mice. *Br. J. Nutr.* **2011**, *105*, 1218−1225.

(13) Mohan, C. G.; Viswanatha, G. L.; Savinay, G.; Rajendra, C. E.; Halemani, P. D. 1,2,3,4,6-Penta-*O*-galloyl-β-D-glucose, a bioactivity guided isolated compound from *Mangifera indica* inhibits 11β-HSD-1 and ameliorates high fat diet-induced diabetes in C57BL/6 mice. *Phytomedicine* **2013**, *20*, 417−426.

(14) (a) Salimifar, M.; Fatehi-Harranabad, Z.; Fatehi, M. A review on natural products for controlling type 2 diabetes with an emphasis on their mechanisms of actions. *Curr. Diabetes Rev.* **2013**, *9*, 402−411. (b) Chang, C. L. T.; Chen, W. C.; Chen, H. M.; Yang, N. S.; Yang, W. C. Natural cures for type 1 diabetes: a review of phytochemicals, biological actions, and clinical potential. *Curr. Med. Chem.* **2013**, *20*, 899−907. (c) Qi, L.; Liu, E.; Chu, C.; Peng, Y. B.; Cai, H. X.; Li, P. Anti-diabetic agents from natural products—an update from 2004 to 2009. *Curr. Top. Med. Chem.* **2010**, *10*, 434−457.

(15) (a) Stefani, M.; Rigacci, S. Protein folding and aggregation into amyloid: the interference by natural phenolic compounds. *Int. J. Mol. Sci.* **2013**, *14*, 12411−12457. (b) Ansari, N.; Khodagholi, F. Natural products as promising drug candidates for the treatment of Alzheimer's disease: molecular mechanism Aspect. *Curr. Neuropharmacol.* **2013**, *11*, 414−429.

(16) Borges, C.; Martinho, P.; Martins, A.; Rauter, A. P.; Ferreira, M. A. A. Characterization of flavonoids extracted of *Genista tenera* by FAB MS/MS. *Rapid Commun. Mass Spectrom.* **2001**, *15*, 1760−1767.

(17) Rauter, A. P.; Martins, A.; Borges, C.; Ferreira, J.; Justino, J.; Bronze, M. R.; Coelho, A. V.; Choi, Y. H.; Verpoorte, R. Liquid chromatography-diode array detection-electrospray ionisation mass spectrometry/nuclear magnetic resonance analyses of the anti-hyperglycemic flavonoid extract of *Genista tenera*. Structure elucidation of a flavonoid-C-glycoside. *J. Chromatogr., A* **2005**, *1089*, 59−64.

(18) Edwards, E. L.; Rodrigues, J. A.; Ferreira, J.; Goodall, D. M.; Rauter, A. P.; Justino, J.; Thomas-Oates, J. Capillary electrophoresis-mass spectrometry characterization of secondary metabolites from the anti-hyperglycemic plant *Genista tenera*. *Electrophoresis* **2006**, *27*, 2164−2170.

(19) Rauter, A. P.; Ferreira, J.; Martins, A.; Santos, R. G.; Serralheiro, M. L.; Borges, C.; Araújo, M. E.; Silva, F.; Goulart, M.; Justino, J.; Rodrigues, J.; Edwards, E.; Thomas-Oates, J. P.; Noronha, J. P.; Pinto, R.; Mota-Filipe, H. Bioactivity studies and chemical profile of the antidiabetic plant *Genista tenera*. *J. Ethnopharmacol.* **2009**, *122*, 384−393.

(20) Rauter, A. P.; Martins, A.; Borges, C.; Mota-Filipe, H.; Pinto, R.; Sepodes, B.; Justino, J. Antihyperglycaemic and protective effects of flavonoids on streptozotocin-induced diabetic rats. *Phytother. Res.* **2010**, *24*, S133−S138.

(21) Rauter, A. P., Jesus, A. R., Martins, A., Dias, C., Ribeiro, R., Macedo, M.-P., Justino, J., Mota-Filipe, H., Pinto, R., Sepodes, B., Medeiros, M., Barbero, J. J., Airoldi, C., Nicotra, F. New C-glycosylpolyphenol antidiabetic agents, effect on glucose tolerance and interactionwith beta-amyloid. Therapeutic applications of the synthesized agent(s) and of *Genista tenera* ethyl acetate extracts containing some of those agents. WO 2013132470A2, 2013 (submitted Mar 9, 2012; publication date, Sep 12, 2013).

(22) Kumazawa, T.; Kimura, T.; Matsuba, S.; Sato, S.; Onodera, J. Synthesis of 8-*C*-glucosylflavones. *Carbohydr. Res.* **2001**, *334*, 183−193.

(23) Sato, S.; Hiroe, K.; Kumazawa, T.; Jun-Ichi, O. Environmentally friendly *C*-glycosylation of phloroacetophenone with unprotected D-glucose using scandium(III) trifluoromethanesulfonate in aquous media: key compounds for the synthesis of mono- and di-*C*-glycosylflavonoids. *Carbohydr. Res.* **2006**, *341*, 1091−1095.

(24) Westermark, P.; Engström, U.; Johnson, K. H.; Westermark, G. T.; Betsholtz, C. Islet amyloid polypeptide: pinpointing amino acid residues linked to amyloid fibril formation. *Proc. Natl. Acad. Sci. U.S.A.* **1990**, *87*, 5036−5040.

(25) Wei, L.; Jiang, P.; Xu, W.; Li, H.; Zhang, H.; Yan, L.; Chan-Park, M. B.; Liu, X.; Tang, K.; Mu, Y.; Pervushin, K. The molecular basis of distinct aggregation pathways of islet amyloid polypeptide. *J. Biol. Chem.* **2011**, *286*, 6291−6300.

(26) (a) Mehla, J.; Chauhan, B. C.; Chauhan, N. B. Experimental induction of type 2 diabetes in aging-accelerated mice triggered Alzheimer-like pathology and memory deficits. *J. Alzheimer's Dis.* **2014**, *39*, 145−162. (b) Kim, B.; Backus, C.; Oh, S.; Feldman, E. L. Hyperglycemia-induced tau cleavage in vitro and in vivo: a possible link between diabetes and Alzheimer's disease. *J. Alzheimer's Dis.* **2013**, *34*, 729−739. (c) Morris, J. K.; Vidoni, E. D.; Honea, R. A.; Burns, J. M. Impaired glycemia and Alzheimer's disease. *Neurobiol. Aging* **2014**, *35*, 585−589.

(27) (a) Mayer, M.; Meyer, B. Characterization of ligand binding by saturation transfer difference NMR spectroscopy. *Angew. Chem., Int.*

Ed. **1999**, *38*, 1784−1788. (b) Mayer, M.; Meyer, B. Group epitope mapping by saturation transfer difference NMR to identify segments of a ligand in direct contact with a protein receptor. *J. Am. Chem. Soc.* **2001**, *123*, 6108−6117. (c) Meyer, B.; Peters, T. NMR spectroscopy techniques for screening and identifying ligand binding to protein receptors. *Angew. Chem., Int. Ed.* **2003**, *42*, 864−890.

(28) (a) Airoldi, C.; Sironi, E.; Dias, C.; Marcelo, F.; Martins, A.; Rauter, A. P.; Nicotra, F.; Jiménez-Barbero, J. Natural compounds against Alzheimer's disease: molecular recognition of Aβ1-42 peptide by *Salvia sclareoides* extract and its major component, rosmarinic acid, as investigated by NMR. *Chem.—Asian J.* **2013**, *8*, 596−602. (b) Airoldi, C.; Cardona, F.; Sironi, E.; Colombo, L.; Salmona, M.; Cambianica, I.; Ornaghi, F.; Sancini, G.; Nicotra, F.; La Ferla, B. Fluorescent amyloid β-peptide ligand derivatives as potential diagnostic tools for Alzheimer's disease. *Pure Appl. Chem.* **2013**, *85*, 1813−1823. (c) Airoldi, C.; Colombo, L.; Manzoni, C.; Sironi, E.; Natalello, A.; Doglia, S. M.; Forloni, G.; Tagliavini, F.; Del Favero, E.; Cantu, L.; Nicotra, F.; Salmona, M. Tetracycline prevents Aβ oligomer toxicity through an atypical supramolecular interaction. *Org. Biomol. Chem.* **2011**, *9*, 463−472. (d) Airoldi, C.; Zona, C.; Sironi, E.; Colombo, L.; Messa, M.; Aurilia, D.; Gregori, M.; Masserini, M.; Salmona, M.; Nicotra, F.; La Ferla, B. Curcumin derivatives as new ligands of Aβ peptides. *J. Biotechnol.* **2011**, *156*, 317−324. (e) Airoldi, C.; Cardona, F.; Sironi, E.; Colombo, L.; Salmona, M.; Silva, A.; Nicotra, F.; La Ferla, B. *cis*-Glyco-fused benzopyran compounds as new amyloid-β peptideligands. *Chem. Commun.* **2011**, *47*, 10266−10268.

(29) *NMR Spectroscopy of Glycoconjugates*; Jiménez-Barbero, J., Peters, T., Eds.; Wiley-VCH: Weinheim, Germany, 2002.

(30) Ni, F.; Zhu, Y. Accounting for ligand−protein interactions in the relaxation-matrix analysis of transferred nuclear Overhauser effects. *J. Magn. Reson. B* **1994**, *103*, 180−184.

(31) Allinger, N. L.; Yuh, Y. H.; Lii, J. H. Molecular mechanics. The MM3 force field for hydrocarbons. 1. *J. Am. Chem. Soc.* **1989**, *111*, 8551−8566.

(32) Qutub, A. A.; Hunt, C. A. Glucose transport to the brain: a systems model. *Brain Res.* **2005**, *49*, 595−617.

(33) Storr, T.; Merkel, M.; Song-Zhao, G. X.; Scott, L. E.; Green, D. E.; Bowen, M. L.; Thompson, K. H.; Patrick, B. O.; Schugar, H. J.; Orvic, C. Synthesis, characterization, and metal coordinating ability of multifunctional carbohydrate-containing compounds for Alzheimer's therapy. *J. Am. Chem. Soc.* **2007**, *129*, 7453−7463.

(34) Ladiwala, A. R. A.; Mora-Pale, M.; Lin, J. C.; Bale, S. S.; Fishman, Z. S.; Dordick, J. S.; Tessier, P. M. Polyphenolic glycosides and aglycones utilize opposing pathways to selectively remodel and inactivate toxic oligomers of amyloid β. *ChemBioChem* **2011**, *12*, 1749−1758.

(35) Zagorski, M. G.; Yang, J.; Shao, H.; Ma, K.; Zeng, H.; Hong, A. Methodological and chemical factors affecting amyloid beta peptide amyloidogenicity. *Methods Enzymol.* **1999**, *309*, 189−203.

(36) *MacroModel*, version 9.6; Schrödinger, LLC: New York, 2008.

(37) *Maestro*, version 9.1; Schrödinger, LLC: New York, 2010.

(38) Martín-Pastor, M.; Espinosa, J. F.; Asensio, J. L.; Jiménez Barbero, J. A comparison of the geometry and of the energy results obtained by application of different molecular mechanics force fields to methyl α-lactoside and the C-analogue of lactose. *Carbohydr. Res.* **1997**, *298*, 15−49.

(39) Still, W. C.; Tempczyk, A.; Hawley, R. C.; Hendrickson, T. Semianalytical treatment of solvation for molecular mechanics and dynamics. *J. Am. Chem. Soc.* **1990**, *112*, 6127−6129.